Schollaen, K., Heinrich, I., Neuwirth, B., Krusic, P. J., D'Arrigo, R. D., Karyanto, O., Helle, G. (2013): Multiple tree-ring chronologies (ring width, δ,13C and δ,18O) reveal dry and rainy season signals of rainfall in Indonesia. - Quaternary Science Reviews, 73, 170-181

DOI: 10.1016/j.quascirev.2013.05.018

Multiple tree-ring chronologies (ring width, $\delta^{13}C$ and $\delta^{18}O$) reveal dry and rainy season signals of rainfall in Indonesia

Karina Schollaen[a*], Ingo Heinrich[a], Burkhard Neuwirth[b], Paul J. Krusic[c], Rosanne D. D´Arrigo[d], Oka Karyanto[e], Gerhard Helle[a]

[a]*GFZ - German Research Centre for Geosciences, Section 5.2 Climate Dynamics and Landscape Evolution, Telegrafenberg, 14473 Potsdam, Germany*

[b]*DeLaWi Tree-Ring Analyses, Preschlinallee 2, D-51570 Windeck, Germany*

[c]*Bert Bolin Centre for Climate Research, Department of Physical Geography and Quaternary Geology, Stockholm University, SE-106 91 Stockholm, Sweden*

[d]*Tree-Ring Laboratory, Lamont-Doherty Earth Observatory, P.O. Box 1000, Route 9W, Palisades, NY 10964, USA*

[e]*Faculty of Forestry, Gadjah Mada University, Yogyakarta, Indonesia*

** Corresponding author.*

Tel.: +49 (0) 331 2881899; Fax: +49 (0) 331 2881302.

E-mail address: karina.schollaen@gfz-potsdam.de.

Abstract

Climatic hazards, such as severe droughts and floods, affect extensive areas across monsoon Asia and can have profound impacts on the populations of that region. The area surrounding Indonesia, including large portions of the eastern Indian Ocean and Java Sea, plays a key role in the global climate system because of the enormous heat and moisture exchange that occurs between the ocean and atmosphere there. Here, we evaluate the influence of rainfall variability on multiple tree-ring parameters of teak (*Tectona grandis*) trees growing in a lowland rain forest in Central Java (Indonesia). We assess the potential of, annually resolved, tree-ring width, stable carbon ($\delta^{13}C$) and oxygen ($\delta^{18}O$) isotope records to improve our understanding of the Asian monsoon variability. Climate response analysis with regional, monthly rainfall data reveals that all three tree-ring parameters are significantly correlated to rainfall, albeit during different monsoon seasons. Precipitation in the beginning of the rainy season (Sep-Nov) is important for tree-ring width, confirming previous studies. Compared to ring width, the stable isotope records possess a higher degree of common signal, especially during portions of the peak rainy season ($\delta^{13}C$: Dec-May; $\delta^{18}O$: Nov-Feb) and are negatively correlated to rainfall. In addition, tree-ring $\delta^{18}O$ also responds positively to peak dry season rainfall, although the $\delta^{18}O$ rainy season signal is stronger and more time-stable. The correlations of opposite sign reflect the distinct seasonal contrast of the $\delta^{18}O$ signatures in rainfall ($^{18}O_{Pre}$) during the dry (^{18}O-enriched rain) and rainy (^{18}O-depleted rain) seasons. This difference in $^{18}O_{Pre}$ signal reflects the combination of two signals in the annual tree-ring $\delta^{18}O$ record. Highly resolved intra-annual $\delta^{18}O$ isotope analyses suggest that the signals of dry and rainy season can be distinguished clearly. Thereby reconstructions can improve our understanding of variations and trends of the hydrological cycle over the Indonesian archipelago.

Highlights

- First well replicated, centennial, multi-parameter TRW, $\delta^{13}C/\delta^{18}O$ record from teak.
- $\delta^{13}C$ and $\delta^{18}O$ records reveal significant higher rainfall signals than tree-ring widths.
- Tree-ring $\delta^{18}O$ responds to peak dry and rainy season rainfall.
- High-resolution $\delta^{18}O_{TR}$ values can distinguish seasonal rainfall variability.
- Reconstruction of seasonal rainfall variability over Indonesia is possible with $\delta^{18}O_{TR}$.

1. Introduction

The climate of Indonesia is governed by an equatorial monsoon system with distinct rainy and dry seasons (e.g. Aldrian and Susanto, 2003; Hastenrath, 1991). Monsoon variations can cause extreme droughts and related wildfires as well as severe flooding, hence, the monsoon has an enormous affect on the livelihood of millions of people (e.g. Boer, 2005). The island of Java, one of the most densely-populated places on the globe, is particularly vulnerable to extremes in rainfall. Understanding long-term, tropical, monsoon variability is crucial since the tropics appear to impact climate worldwide (e.g. Evans et al., 2001; Sarachik and Cane, 2010; Ummenhofer et al., 2013). However, instrumental climate data in this area are spatially and temporally limited. High-resolution proxy records would improve considerably our understanding of past monsoon variations.

Tree rings are one of the most important archives in palaeoclimate research because of their precisely dated, annually resolved information, and the broad geographical distribution of trees (Hughes, 2011). Previous studies in Asia have revealed relationships between tree-ring width and climate parameters such as rainfall (e.g. Berlage, 1931; Pumijumnong et al., 1995; Ram et al., 2008), sea surface temperature (e.g. D'Arrigo et al., 2006b) or monsoon related parameters like drought frequency and intensity (e.g. Borgaonkar et al., 2010; Buckley et al., 2007). However, no land rainfall reconstruction from tree-ring width indices exists for the Indonesian Archipelago.

Tree rings not only record growth rates as measured in ring widths, but also provide stable isotope ratios that are directly controlled by a range of external and internal factors that are reasonably well understood (Barbour, 2007; Farquhar et al., 1982; Helle and Schleser, 2004b; McCarroll and Loader, 2004; Roden et al., 2000). Therefore, it is reasonable to expect tree-ring stable isotope records could provide climate information beyond that contained in ring widths.

The carbon and oxygen isotope composition in tropical tree rings contains information about hydrological changes in the arboreal system. $\delta^{13}C$ has mainly been used to study changes in intrinsic water-use efficiency of trees, as well as physiological responses to climatic changes (e.g. Brienen et al., 2011; Cernusak et al., 2007; Fichtler et al., 2010; Gebrekirstos et al., 2009; Hietz et al., 2005; Nock et al., 2011). $\delta^{18}O$ in tropical timber has been proven to primarily represent the isotopic composition of rain, i.e. the source-water (e.g. Brienen et al., 2012; Evans and Schrag, 2004). Plant physiological effects like leaf water enrichment due to transpiration (Barbour, 2007; Helle and Schleser, 2004b; McCarroll and Loader, 2004; Roden et al., 2000) do not seem to be particularly pronounced in $\delta^{18}O$ records from tropical tree rings (e.g. Brienen et al., 2012). Variation of $\delta^{18}O$ in rainfall is determined by several factors where the amount of rain (Araguás-Araguás et al., 1998; Dansgaard, 1964) plays a key role in producing a strong inverse correlation (Fig. 2A).

The majority of tree-ring oxygen isotope studies from lowland tropics undertaken so far, relies on just a few replicated samples (1-3), and mostly reveals the expected significant negative correlation with rainfall amounts (Ballantyne et al., 2010; Evans, 2007; Evans and Schrag, 2004; Managave et al., 2011; Poussart et al., 2004), although in one instance a positive correlation with rainfall amount was found (Managave et al., 2010b). From tropical or sub-tropical Asia centennial, or even longer, stable isotope records are scarce (e.g. Managave et al., 2011; Sano et al., 2012; Zhu et al., 2012). To date no well replicated, long-term, stable isotope record exists from lowland teak trees.

In this study, we present the first well-replicated centennial stable isotope records ($\delta^{13}C_{TR}$ and $\delta^{18}O_{TR}$) for Indonesia derived from teak. We selected a site for isotope analyses previously reported to have a rather weak ring width climate signal (D'Arrigo et al., 2006b). The aim was to test if tree-ring stable isotopes reveal a better relationship to rainfall than ring widths. Hence, we compared carbon and oxygen isotopes ($\delta^{13}C_{TR}$, $\delta^{18}O_{TR}$), as well as tree-ring width (TRW) chronologies from the same

material to regional monthly rainfall data and seasonal sums of monthly rainfall in order to assess isotopic variability on inter-annual scales. Finally, we use highly resolved intra-annual $\delta^{18}O_{TR}$ data to explain the transfer of the $\delta^{18}O$ rainfall signal ($\delta^{18}O_{Pre}$) of dry and rainy season into the tree rings of teak to prove potential additional value of isotope analyses for climate investigations.

2. Material and methods

2.1. Regional setting

Teak samples were collected from a lowland rain forest at an elevation of 380 m a.s.l. The study site, named Donoloyo, is located 90 km east of the city of Yogyakarta in the eastern part of Central Java, Indonesia (07°52'S, 111°11'E) (Fig. 1). The same site was part of an earlier investigation on teak tree-ring width described in D'Arrigo et al. (2006a,b). This study site is a very old forest and for the last few decades, a protected area. In former times only selected timber were taken from this forest for the construction of palaces and mosques.

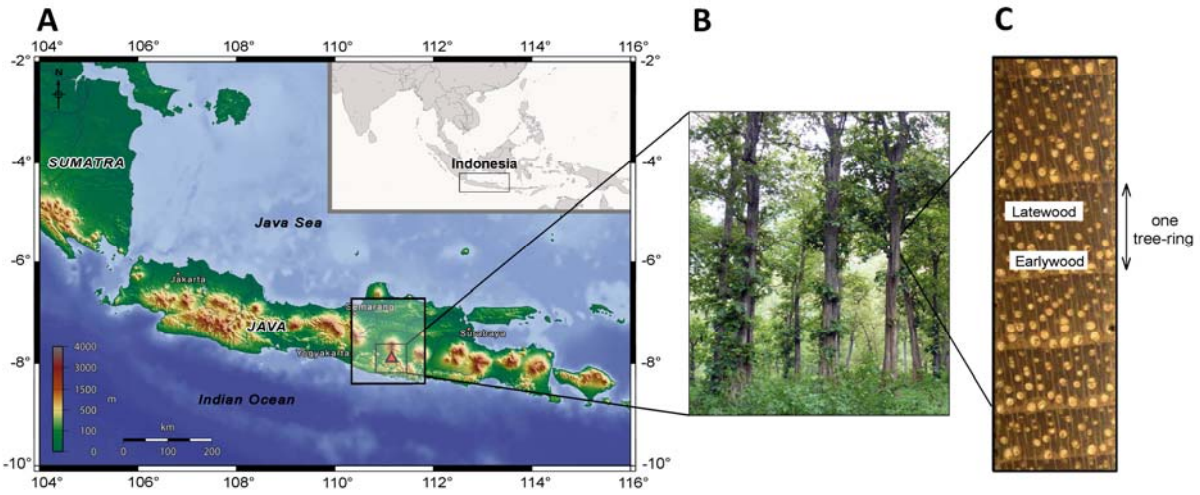

Fig. 1. (A) Map showing the location of the study site in a lowland rain forest (380 m a.s.l.) in the eastern part of Central Java (07°52'S, 111°11'E). (B) Photograph shows the study site (Donoloyo) with teak (*Tectona grandis*) trees. (C) Microscopic image showing wood anatomical structure of a teak cross section from the study site.

Most of the Indonesian archipelago receives rainfall throughout the year and encompasses a variety of rainfall regimes (Braak, 1921-29). However, Central and Eastern Java are influenced by the equatorial monsoon climate, characterized by distinct rainy and dry seasons (Fig.2A). The rainy season begins with the arrival of the north-west monsoon in October and normally persists till May of the following year. The dry season follows the south-east monsoon from June to September. The peak of the rainy season is centred between December and February, when a quasi-permanent low-pressure centre over the region develops and lower-tropospheric convergence is pronounced. More detailed information about the meteorology of Indonesia can be found in Sukanto (1969), Hackert and Hastenrath (1986) and McBride (1999).

The isotopic composition of rainfall over Java shows distinct seasonal changes linked to rainfall amount. Rainfall during the dry season (~200 mm on average (Jun-Sep), 1900-2002) is generally enriched in ^{18}O (less negative $\delta^{18}O_{Pre}$ values). This is a consequence of reduced condensation processes that leads to a "heavy" isotope composition in rainfall. Relative to the dry season, rain during the rainy season (~1700 mm on average (Oct-May), 1900-2002) is generally much more

depleted in ^{18}O (more negative $\delta^{18}O_{Pre}$ values) due to extended, cumulative, rainout processes (Araguás-Araguás et al., 2000; Dansgaard, 1964; Gat, 1996). Data on the $\delta^{18}O$ of rain water is available from the "Global Network of Isotopes in Precipitation (GNIP)" maintained by the International Atomic Energy Agency (IAEA), Vienna. The closest GNIP station to our study site is ca 500 km away, near Jakarta. It provides data from 1962 to 1998. The seasonal rainfall pattern and amount recorded at this station are similar to that at Donoloyo (Fig. 2A, grey line).

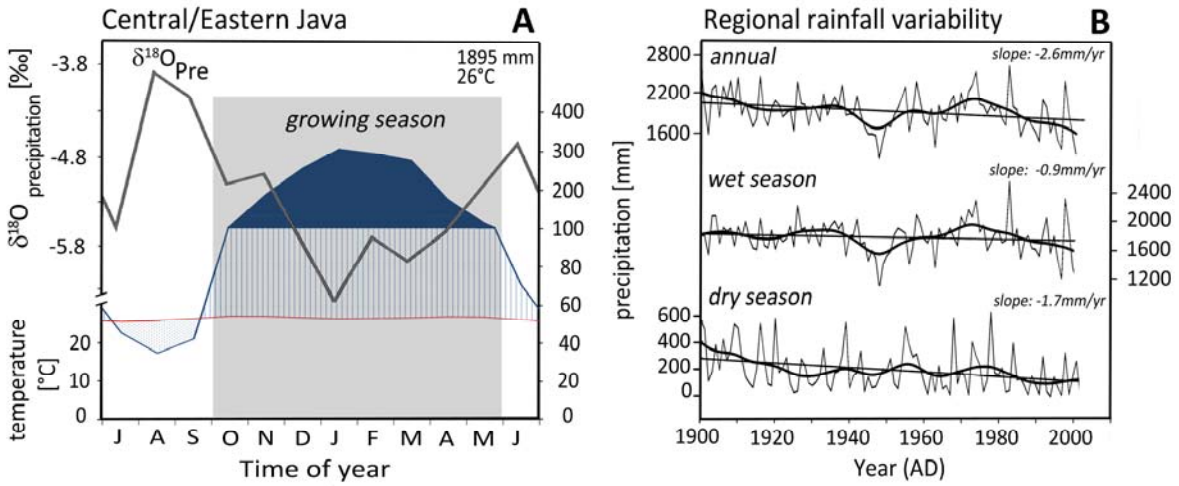

Fig. 2. (A) Mean monthly rainfall and temperature at the study site derived from a regional mean (REG) of different stations for rainfall (1900-2002; see Supplementary Table A/Fig. A) and gridded climate data for temperature (CRU3.0 1901-2002; Mitchell and Jones, 2005). Grey line indicates the monthly mean $\delta^{18}O$ values in rainfall ($\delta^{18}O_{Pre}$) for Jakarta/Indonesia (1962-1998; GNIP: http://www-naweb.iaea.org). The growing season (grey shadow) of teak extends approximately from October to May. At rainfall levels above 100 mm the axis scale is shortened (Walter and Breckle, 1991). (B) Regional rainfall for rainy (October to May) and dry (June to September) season and annual sum (REG, 1900-2002). 20-year cubic-smoothing splines (thick black lines) and linear trend lines (black lines) show long-term fluctuations and trends.

The amount of rainfall in the region of our study site shows a declining long-term trend (1900-2002) in the annual rainfall sum (-2.7 mm per year), with the dry season showing a very high and almost linear decrease (-1.7 mm per year) over the 20th century (Fig. 2B). The rainy season is characterized by rather stable rainfall conditions from 1900 to 1940, a drastic decline during the 1940s, followed by increasing rainfall from 1950 to 1974. Since the late 1970s, total annual rainfall has decreased with higher year-to-year variability then previously recorded. The severe decline from 1945 to 1950 may be due to the drastic decrease in the number of reporting meteorological stations during the Indonesian National Revolution that occurred at the same time (see Supplementary Fig. B). Overall, since 1900, there has been a general trend towards drier conditions in Central/Eastern Java.

The vegetation period (growing season) for teak in Central and Eastern Java generally lasts from the beginning of October to the end of May (Coster, 1927, 1928; Geiger, 1915). From about mid-June to September (dry season) the trees are leafless and produce no wood as they are in a state of cambial dormancy (Coster, 1927, 1928). Bud burst and cambial activity start with the onset of the monsoon rains and flowering occurs towards the end of the rainy season. Thus teak is showing distinct annual growth rings, mainly due to the seasonality of rainfall in their habitat.

2.2. Ring-width chronology

The ring-width (TRW) chronology for this study site was developed from 32 wood cores of 16 teak trees (2 cores per tree, 5 mm diameter). Eight of the 16 trees were collected during a field campaign in November 2008 and another eight drawn from a collection used in a previous study by D'Arrigo and co-workers (D'Arrigo et al., 2006b). All pre-treatment of the collected samples was carried out in the laboratory following standard procedures outlined in Stokes and Smiley (1968) and Schweingruber (1983). To improve the visibility of the tree-ring structure the surface of the core samples was cut with a microtome (WSL core microtome, Switzerland) and fine chalk was rubbed into the pores to increase ring contrast. For dating purposes, we followed the convention for the southern hemisphere, which assigns to each tree ring the year in which radial growth begins (Schulman, 1956). Subsequently, ring widths were measured and synchronized with the program TSAPWin (Rinn, 2005) using statistical tests (Gleichläufigkeit, t-test). Visual crossdating (Fritts, 1976) was performed by skeleton plots (Douglass, 1935) and verified using COFECHA software (Holmes, 1983). We used the program ARSTAN (Cook et al., 2012) for standardization and chronology construction. The individual raw ring-width series were standardized by fitting a cubic smoothing spline (Cook and Peters, 1981) with a 50% frequency response cut-off at 67% of the series length to each TRW series to remove age trends. Indices were calculated as ratios between the measured ring-widths and spline values. The resulting standardized index values were prewhitened using an autoregressive model, then averaged across all series using a be-weight robust mean to reduce the influence of outliers (Cook and Kairiukstis, 1990).

2.3. $\delta^{13}C_{TR}$ and $\delta^{18}O_{TR}$ chronologies

For dendroclimatic isotope studies four to six trees are considered sufficient (e.g. Leavitt, 2010). In this experiment we used seven different trees chosen according to the following criteria: (i) correct dating and highly correlated measurements with the master reference curve developed from all trees in the study (indicated by statistical parameters such as Gleichläufigkeit-values) (Cropper, 1979; Riemer, 1994; Schweingruber et al., 1990) and Pearson's correlation coefficient (Briffa and Jones, 1990; Wigley et al., 1984), (ii) distinct and straight tree-ring borders and (iii) fewest number of problematic zones containing such features as false, narrow or missing rings. We analysed 108 years (1900-2007), a period long enough to provide sufficient calibration and verification with instrumental climate data, and reveal potential trends over the 20th century. The tree rings from all cores were separated individually with a scalpel and ground to assure homogeneity. Extractives, such as wood resins and oils, but also glue, pencil and chalk remains were removed from the wood with boiling de-ionized water and ethanol in a multiple sample isolation system for solids (Wieloch et al., 2011). Recent research has shown that the cellulose extraction is not as crucial as previously thought 30-40 years ago (Borella et al., 1998; McCarroll and Loader, 2004; Taylor et al., 2008; Verheyden et al., 2005). Hence, resin extracted wood material was used instead of cellulose due to some very narrow rings which would not have provided sufficient amounts of cellulose for conventional online Isotope Ratio Mass Spectrometer (IRMS) determination of $\delta^{13}C$ and $\delta^{18}O$. Carbon isotope ratios were measured by combustion (at 1080°C) using an elemental analyser (Model NA 1500; Carlo Erba, Milan, Italy) coupled online to an IRMS (Isoprime Ltd. Cheadle Hulme, United Kingdom). Oxygen isotope ratios were measured using a high temperature TC/EA pyrolysis furnace (at 1340°C) coupled online

to an IRMS (Delta V Advantage, Thermo Scientific, Bremen, Germany). Sample replication resulted in a reproducibility of better than ±0.1‰ for $\delta^{13}C_{TR}$ values and ±0.25‰ for $\delta^{18}O_{TR}$ values. The isotope ratios are given in the conventional delta (δ) notation, relative to the standards VPDB for $\delta^{13}C$ and VSMOW for $\delta^{18}O$ (Craig, 1957).

The carbon isotope record was corrected for anthropogenic changes in atmospheric CO_2 induced by fossil fuel burning and deforestation since industrialization (1850). A decline in the atmospheric $\delta^{13}C$ source was removed from the raw $\delta^{13}C_{TR}$ series by subtracting for each tree-ring stable isotope value the annual changes in $\delta^{13}C$ of atmospheric CO_2 obtained from ice cores and direct measurements (Leuenberger, 2007) resulting in a corrected $\delta^{13}C$ record ($\delta^{13}C_{cor1}$). To take account of changes in plant response potentially from increasing atmospheric CO_2 concentrations (pCO_2), a further correction was applied. Since this plant physiological effect is under debate, we show a range of published pCO_2 effects on $\delta^{13}C_{TR}$ (Feng and Epstein, 1995; Kürschner et al., 1996; Schubert and Jahren, 2012). For further data analysis we chose a moderate correction for pCO_2 effects on carbon isotope discrimination of 0.73‰ per 100 ppm ($\delta^{13}C_{Cor2}$; Kürschner et al., 1996; Schubert and Jahren, 2012). No corrections are required for the oxygen isotope data.

2.4. High-resolution intra-annual sampling of tree rings

High-resolution intra-annual sampling was performed by using an UV-Laser microdissection microscope (LMD7000, LEICA Microsystems, Wetzlar, Germany). First, cross-sections from the wood cores (5 mm diameter) were cut with a core microtome (Gärtner and Nievergelt, 2010). Second, the cross-sections (approximately 500 µm thickness) were fixed in special metal frame slides and mounted on the object holder of the microdissection microscope. The annual rings were graphically subdivided into several sub-sections in a radial direction with a pen screen. The number of sub-sections per ring varied depending on the tree-ring width and the size of dissected wood tissue. Every sub-section defined on the pen screen was dissected with the UV-laser beam and collected in a single silver capsule standing in a collection holder. The capsules were sealed and put onto an autosampler of a high temperature pyrolysis furnace coupled online to an IRMS.

2.5. Climate data and data treatment

The study site has a typical equatorial climate with rather stable temperature but notably variable rainfall (dry/rainy season) (Fig. 2A). Hence, climate calibration was performed using rainfall data. We screened monthly rainfall data for more than 40 meteorological stations and selected 17 stations for calibration purposes based on the distance to the study site, number of missing values and length of measurements (Supplementary Table A). All the selected meteorological stations (KNMI Climate Explorer: http://climexp.knmi.nl/) show the characteristic monsoonal rainfall pattern for Central and Eastern Java (Fig. 2A) and a regional mean of rainfall series (REG; Supplementary Fig. B) was calculated (Jones and Hulme, 1996). The period 1900–2002 (103 years) was used for the climate versus tree-ring correlation analyses. In order to investigate the climate-proxy relationships we calculated Pearson‘s correlation coefficients between tree-ring parameters (TRW, $\delta^{13}C_{TR}$, $\delta^{18}O_{TR}$) and climate data on a monthly basis. For time scale units we followed the vegetation period as opposed to a calendar perspective. Thus a year lasts from October (start of growing season) to September of the following calendar year.

To test the temporal stability of rainfall on the tree-ring parameters, running correlations between the monthly climate records and the tree-ring series, over a 31 year time window, were calculated.

3. Results

3.1. Site chronologies

The TRW series from 16 trees agree reasonably well (expressed population signal (EPS) of 0.94, GLK=63%, Table 1). The year-to-year variability changes over time with low values at the beginning of the chronology (18th century) and greater variability over the 19th and 20th century (Fig. 3A/B). The carbon isotope series show a low year-to-year variability (Fig. 3C/D). The mean inter-series correlation after correcting for changing atmospheric $\delta^{13}CO_2$ values is relatively low (r=0.27), as well as the EPS value (EPS=0.72). However, the inter-series correlation and EPS increase after correction for the pCO_2 effect ($\delta^{13}C_{cor2}$: r=0.36, EPS=0.80, Table 1). In contrast to $\delta^{13}C$, the oxygen isotopes ($\delta^{18}O$) from the same seven individuals are well correlated (Fig. 3E) and show a high degree of synchronization (r=0.55, GLK=70%, EPS=0.90, Table 1). Furthermore, the $\delta^{18}O_{TR}$ variance is stable throughout the entire 20th century and the mean year-to-year variability of $\delta^{18}O_{TR}$ is higher than of the $\delta^{13}C_{TR}$ record.
Interestingly, the chronologies of all three parameters show more or less the same multi-decadal long-term changes beginning with a declining trend during 1910-1930 followed by increasing values (1930-1960) and an obvious rising trend towards the end of each record (1990-2007).

Table 1. Descriptive statistics for the tree-ring width (TRW), $\delta^{13}C_{TR}$ and $\delta^{18}O_{TR}$ chronologies. $\delta^{13}C_{TR}$ series include correction for changing atmospheric $\delta^{13}CO_2$ ($\delta^{13}C_{cor1}$:Leuenberger, 2007) and for changing plant response to increasing atmospheric CO_2 concentration ($\delta^{13}C_{cor2}$: Kürschner et al., 1996; $\delta^{13}C_{cor3}$: Feng and Epstein, 1995). CL: length of chronology; SD: standard deviation; GLK: Gleichläufigkeit (Cropper, 1979; Esper et al., 2001); Corr: series intercorrelation; EPS: expressed population signal (Wigley et al. 1984); AC1: autocorrelation first order; Inter-series corr: mean inter-series correlation.

	Time-span	CL	Nr. of trees	mean	SD	GLK [%]	corr	EPS	AC1	Inter-series corr
TRW	1714-2007	294	16	1.01	±0.24	63	0.48	0.94	0.31[a]	0.26 ($\delta^{13}C_{cor2}$)
$\delta^{13}C_{TR}$										
$\delta^{13}C_{cor1}$	1900-2007	108	7	-25.22	±0.34	61	0.27	0.72	0.62	
$\delta^{13}C_{cor2}$	1900-2007	108	7	-24.94	±0.41	61	0.36	0.80	0.72	0.25 ($\delta^{18}O_{TR}$)
$\delta^{13}C_{cor3}$	1900-2007	108	7	-24.46	±0.61	62	0.59	0.91	0.88	
$\delta^{18}O_{TR}$	1900-2007	108	7	21.17	±0.62	70	0.55	0.90	0.22	0.28 (TRW)

[a] Autocorrelation of Arstan standard chronology

3.2. Inter–annual tree response to rainfall

Simple linear correlation coefficients between the tree-ring series and monthly mean rainfall totals are shown from, the start of growing season, October, to September of the following year (Fig.4 and Table 2). The climate response between rainfall and tree-ring width (Fig. 4A) shows significant positive correlations with the previous transitional month of May (pMay, r=0.26) and the previous dry season (pJun to pSep), as well as with the beginning of the rainy season, where the sum of September to November rainfall shows the highest correlation (r=0.27, p<0.01, Table 2). However, the strength and sign of the September to November correlation is not stable for the observed time period. The relationship falls below the significance level from 1920 to 25 and 1960 to 75, and changes sign during the latter (right plot in Fig. 4A, Table 2).

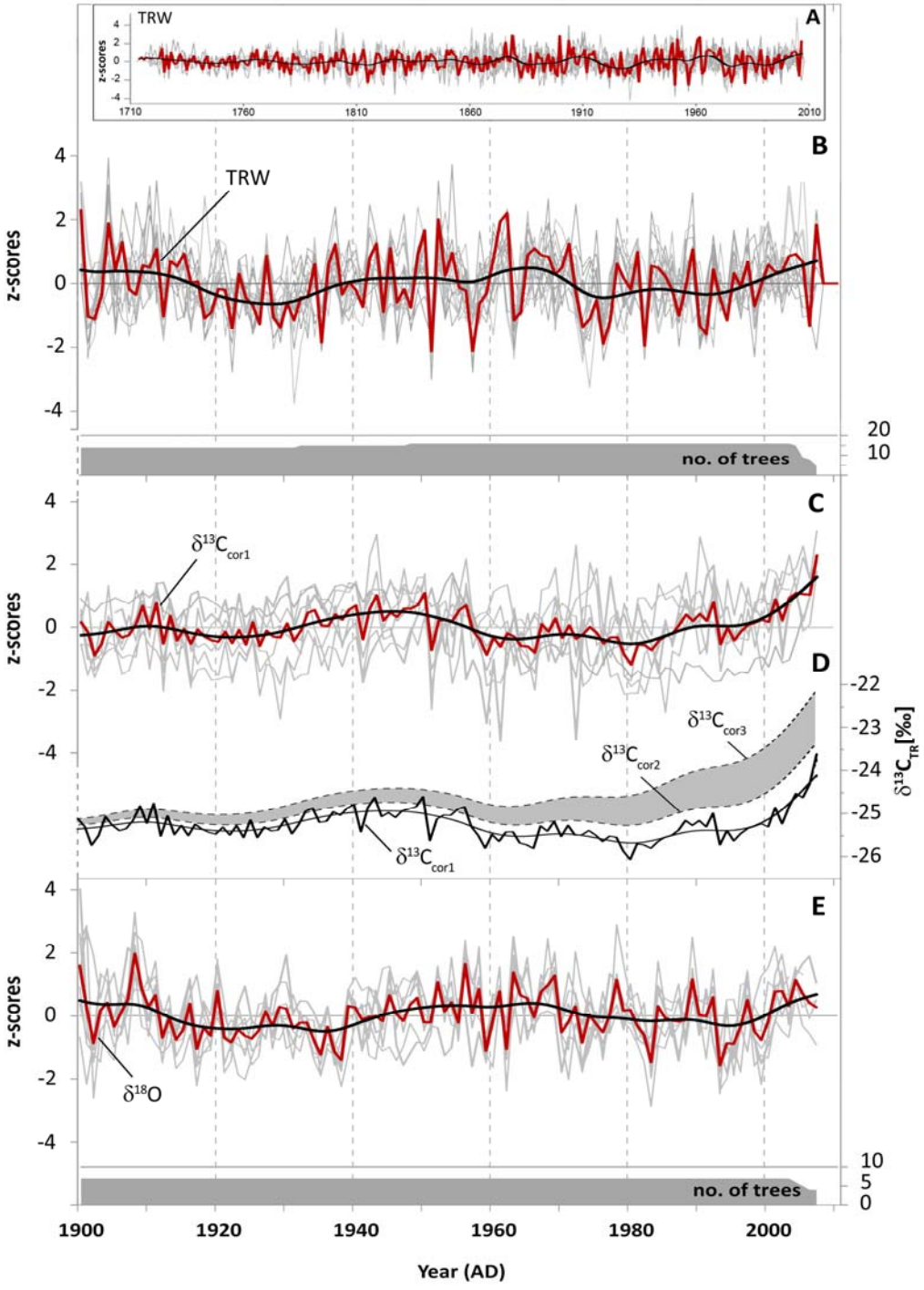

Fig. 3. Tree-ring series of ring width, $\delta^{13}C$ and $\delta^{18}O$ (red lines represent the mean chronology of each parameter). (A/B) Detrended tree-ring width series; (C/D) Corrected carbon isotope series: (C) Raw data corrected for changing $\delta^{13}C$ of atmospheric CO_2 ($\delta^{13}C_{Cor1}$, thick red line), data after (Leuenberger, 2007), (D) Carbon isotopic data ($\delta^{13}C_{Cor1}$, thick black line) corrected for potential plant isotopic response to increasing atmospheric CO_2 concentration ($\delta^{13}C_{cor2}/_{cor3}$, grey shaded area). Grey shaded area envelopes the minimum/maximum range of pCO_2 correction according to literature ($\delta^{13}C_{cor2}$: Kürschner et al., 1996; $\delta^{13}C_{cor3}$: Feng and Epstein, 1995); (E) Oxygen isotope series. 20-year cubic-smoothing splines (thick black lines) fitted on the chronologies are depicted to show long-term fluctuations. Sample depths are shown as grey areas at the bottom of each graph (right axis).

The $\delta^{13}C_{TR}$ chronology (Fig. 4B) shows a highly significant negative relation to the current rainy season, with December to May rainfall exhibiting the highest influence (Dec-May r=-0.41, p<0.001, Table 2). The negative signal is stable from 1935 to 1970 (right plot in Fig. 4B, Table 2).
$\delta^{18}O_{TR}$ generally shows significant positive and negative correlations with rainfall of the prior dry season (pJun-pSep) and with the current rainy season (growing period), respectively (Fig. 4C, Table 2). In the dry season only the month of August, which is the driest month of the year, showed a highly significant correlation (r=0.40, p<0.001, Table 2) with the $\delta^{18}O_{TR}$ record. During the rainy season it is the rainfall during the peak of rainy season (November to February) that shows the highest significant correlation (r=-0.40, p<0.001, Table 2). This rainy season signal is stable for the entire time period after 1920, whereas the positive signal of the peak of the dry season (August) is significant only before 1940 and after 1975 (right plot in Fig. 4C). Seasonality, as reflected by the difference in rainfall between August and January, as well as between the most significant months of the prior dry season (pJun-pSep) and the peak rainy season months (Nov-Feb) reveals highly significant correlations (r=0.4 and r=0.53, p<0.001) and are stable over the whole 20th century. Correlations between the tree-ring $\delta^{18}O$ and the annual $\delta^{18}O_{Pre}$ values from the GNIP station in Jakarta (1962-1998, Fig. 2A) show significant positive values (mean r=0.45, p<0.05), where 2 out of 7 tree-ring $\delta^{18}O$ series indicate highly significant correlations (r=0.63, p<0.01).

Table 2. Pearson correlation coefficients between tree-ring parameters (TRW, $\delta^{13}C_{TR}$, $\delta^{18}O_{TR}$) and rainfall data for different time periods (*p<0.05, **p<0.01, ***p<0.001).

Tree-ring parameter	Time period	Annual[a]	Dry season[b]	Wet season[c]	Period of strongest relationship
TRW	1900-2002	0.10	0.22	-0.02	0.27** (pSep-Nov)
	1900-1924	0.44	0.50*	0.14	0.58*** (pMay-pSep)
	1925-1949	-0.02	0.41*	-0.12	0.41* (dry season)
	1950-1974	-0.17	-0.35	-0.03	-0.35 (dry season)
	1975-2002	0.03	0.38*	-0.11	0.44* (pJul-Nov)
$\delta^{13}C_{TR}$	1900-2002	-0.29**	-0.03	-0.32***	-0.41*** (Dec-May)
	1900-1924	0.11	0.30	-0.06	0.40* (pMay-pJun)
	1925-1949	-0.34	0.30	-0.45*	-0.61** (Dec)
	1950-1974	0.02	0.23	-0.21	-0.49* (Jan)
	1975-2002	-0.41*	-0.08	-0.35	-0.44* (Dec-Jan)
$\delta^{18}O_{TR}$	1900-2002	-0.04	0.35***	-0.27**	-0.40*** (Nov-Feb); 0.40***(pAug) 0.53***(Diff. dry-wet season)
	1900-1924	0.70***	0.71***	0.28	0.76*** (pJul-pAug)

1925-1949	-0.51**	0.13	-0.54**	-0.54** (wet season)
1950-1974	-0.37	-0.12	-0.43*	-0.73*** (Nov-Feb)
1975-2002	-0.33	0.47*	-0.50**	-0.52** (Nov-Feb)

[a] Annual= July to June next year**.**

[b] Dry season= pJune to pSeptember.

[c] Wet season= October to May.

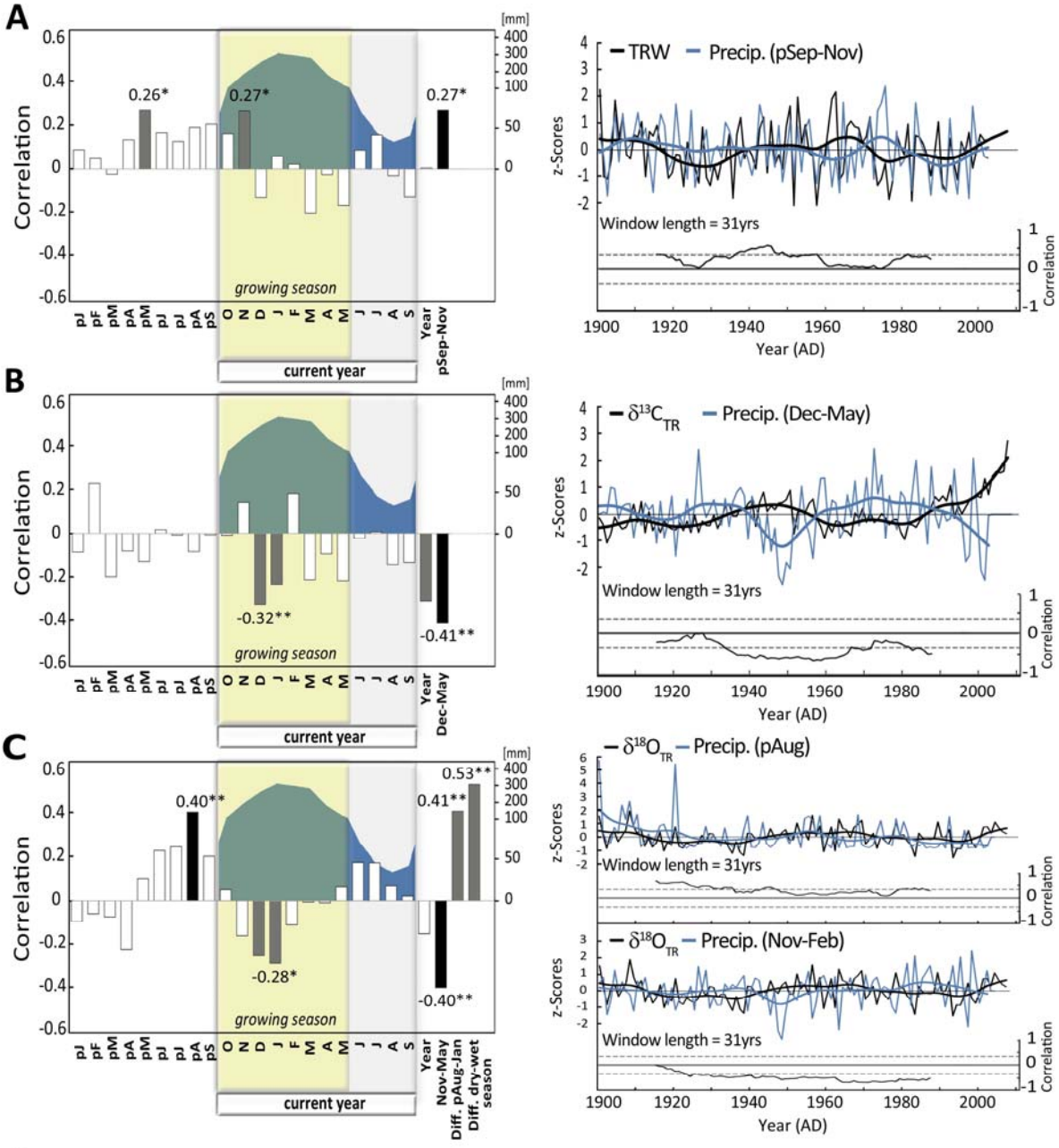

Fig. 4. Left: Correlations of (A) TRW, (B) $\delta^{13}C_{TR}$ and (C) $\delta^{18}O_{TR}$ chronologies with monthly and seasonal rainfall (1900-2002). The climate response plots are separated into three parts by vertical lines. The left part covers months of the previous year (previous year January to September) followed by the current year (October to following year September). The right part depicts seasonal means. Long-term seasonal average of rainfall is shown as blue shaded area in the background. Most significant

correlations are indicated with grey bars, where highest correlations are highlighted in black (**p<0.001,* p<0.01). Right: Time series of tree-ring parameters and corresponding rainfall of periods with highest influence. Moving correlations for overlapping 31-year periods (95% confidence levels are indicated) and 20-year cubic smoothing spline (thick blue and black lines) are shown.

3.3. Intra-annual cyclicity in high-resolution $\delta^{18}O_{TR}$ records

The opposite correlations found for the tree-ring $\delta^{18}O$ and monsoonal rainfall amount of dry and rainy season, respectively, are conspicuous. Highly resolved intra-annual $\delta^{18}O_{TR}$ data may help to understand the observed relations. Figure 5B shows growing season $\delta^{18}O_{TR}$ profiles at various numbers of sub-sections per year from one teak tree. Consecutive $\delta^{18}O_{TR}$ values are plotted relative to their positions within the rings formed in 1983, '84 and '86. The $\delta^{18}O_{TR}$ profiles reveal a clear annual cycle. Annual wood formation starts with a parenchyma band having $\delta^{18}O_{TR}$ values that are similar to the $\delta^{18}O_{TR}$ values at the end of the previous tree ring. Wood being formed shortly after the parenchyma band is characterized by rapidly rising $\delta^{18}O_{TR}$ values up to the ring maximum early in the growing season. After the maximum is reached, $\delta^{18}O_{TR}$ values decline to a seasonal minimum typically in the 2nd third of each tree ring before $\delta^{18}O_{TR}$ slightly rises again in the last third of the growing season. The pattern described here was found rather consistent in spite of the different numbers of intra-annual data points, i.e. sub-sections per year. However, this shows that the number of intra-ring data points can affect the variance of intra-annual $\delta^{18}O_{TR}$ and complicates the climatic interpretation of such data.

4. Discussion

4.1. Tree-ring parameters and their rainfall signals

Climate correlation tests showed that all three tree-ring parameters are significantly influenced by seasonal rainfall amounts. The correlations of stable isotope records with rainfall were mostly significant and constant over time. The 300-year long TRW chronology produced similar correlation patterns with rainfall as found in previous Javanese teak studies (Berlage, 1931; D'Arrigo et al., 1994; DeBoer, 1951; Jacoby and D'Arrigo, 1990; Murphy et al., 1989). However, the TRW chronology did not reveal stable correlations with regional rainfall data sets. Previous authors concluded that teak growth is positively correlated with rainfall in the prior dry season (around May to September), but mainly controlled by the transitional months of the corresponding monsoons, May/June and October/November. Teak studies from Thailand (Buckley et al., 2007; Pumijumnong et al., 1995) likewise note that rainfall at the beginning of the wet monsoon is the most significant climate factor controlling tree-ring growth, whereas Indian studies reveal significant positive relationships with rainfall over the whole Indian Summer Monsoon season (Borgaonkar et al., 2010; Shah et al., 2007) and annual total rainfall (Ram et al., 2008).

The negative relationship found between $\delta^{13}C_{TR}$ and the main rainy season (Dec-May) is well in line with the theories of carbon isotope discrimination during photosynthesis and seasonal changes in post-photosynthetic signal transfer from the leaf level into the developing wood tissue (e.g. McCarroll and Loader, 2004). Contrary to the TRW data, $\delta^{13}C_{TR}$ reveals no significant correlation with the very early growing season. Why? At the very beginning of the growing season, i.e. rainy season, early wood formation relies on assimilates from previous years, accumulated as starch reserves. Previous year's starch is not necessarily isotopically labelled by the climate signal of its formation

period. It rather exhibits a general enrichment of ^{13}C as compared to less polymerized assimilates. Consequently, the incorporation of starch derived ^{13}C masks a potential early growing season climate signal of tree-ring $\delta^{13}C$ (e.g. Helle and Schleser, 2004a) and could not be found in this study. With the progressing growing season, developing leaves subsequently provide new assimilates for wood growth, which carries the signal of the current growing season in their $\delta^{13}C_{TR}$. As the temperatures at our study site are quite stable over the entire year it is likely that stomatal conductance driven by varying stomatal aperture in response to moisture supply is controlling the c_i/c_a ratio and finally resulting in the observed significant negative correlation between tree-ring $\delta^{13}C$ and the rainfall of the Dec-May period (main rainy season). However, too much rain during this period of the year may weaken the relationship as revealed by decreased correlations during wet phases around 1920-30 and 1970-80 (Fig. 4B, Fig. 2B).

The $\delta^{18}O_{TR}$ record shows stable inverse relation with the November to February interval of the rainy season, i.e. the wettest period of the year, and a notable significant positive correlation with the rainfall of prior driest month August. Interestingly, the correlation of tree-ring $\delta^{18}O$ with rainfall is significant during those months of the year that are generally characterized by both the highest and the lowest $\delta^{18}O$ values in rainfall (Fig. 2A). This is because the source water signal of the soil is dominated by the seasonally changing $\delta^{18}O$ signature in rainfall that is highest during the peak of the dry season (August) and lowest during the peak of the rainy season (January). Any influence of groundwater due to uptake from deeper soil reservoirs during the vegetation period seems unlikely since the volcanic soil substrate at the site is well-drained and teak has a shallow root system. Thus, tree-ring $\delta^{18}O$ in teak provides rainy and dry season signal of $\delta^{18}O$ in rainfall. This is emphasized by the significant positive correlation found between the tree-ring $\delta^{18}O$ and the annual $\delta^{18}O_{Pre}$ values from the GNIP station in Jakarta. The finding suggests that the $\delta^{18}O_{TR}$ signal may be coherent over larger areas. During the first 25 years of the 20th century our $\delta^{18}O_{TR}$ has the highest (positive) correlation with dry season rainfall in contrast to the high negative correlation with the main rainy season (Nov-Feb) during the remaining part of the 20th century (Fig. 4C, Table 2). This may result from the wetter conditions particularly prevailing during the dry seasons of the first 25 years of the 20th century (Fig. 2B), which strengthens the dry season signal in the tree-ring $\delta^{18}O$. Such shifts in intra-annual tree-ring proxy response to changing rainfall conditions cannot be detected or confirmed without independent proxy or instrumental data sets. However, intra-annual stable isotope data from tree rings can help to disentangle contrasting isotopic effects of dry and rainy season rainfall amount.

4.2. Rainfall signals in tree-ring $\delta^{18}O$ as a function of the hydrological seasonal cycle

High-resolution intra-ring $\delta^{18}O$-records (Fig. 5B) give more detailed insight into the seasonal hydrological cycle and its effects on tree-ring $\delta^{18}O$. Our observations largely corroborate those outlined by Evans and Schrag (2004) for evergreen tropical species without distinct tree rings. Lower intra-annual $\delta^{18}O_{TR}$ values correspond to periods of higher rainfall with lower evapotranspiration and vice versa. However, how can a dry season influence the tree-ring $\delta^{18}O$ of a deciduous species that is leafless and does not grow at all during this period of the year? To explain this we adapted in Fig. 5A a conceptual oxygen isotope model to the hydrological conditions at our study site for comparison. During the dry season no leaf transpiration and photosynthesis occurs, and no wood is formed. Consequently, no direct impact of the prevailing hydrological conditions can be expected. However, the rain water that is potentially seeping into the soil is enriched in ^{18}O due to reduced condensation

processes (Jun–Sep, long-term mean 1900-2002: 200 mm, range: 0-628 mm, $\delta^{18}O_{Pre}$= -3.8‰) and possibly high soil water evaporation rates promoted by direct insolation. This leads to ^{18}O-enrichment in soil water that culminates shortly before the beginning of the growing period.

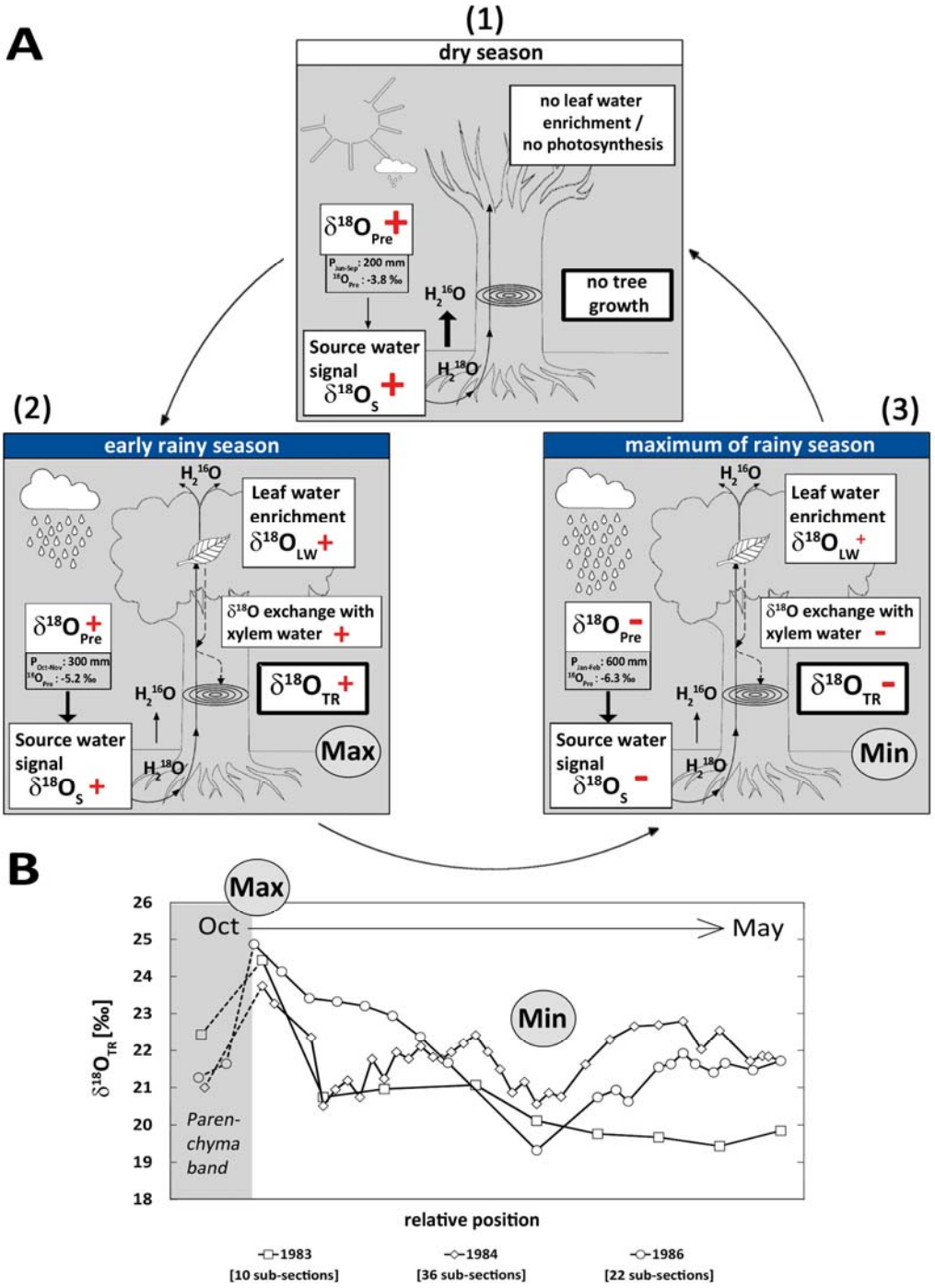

Fig. 5. (A) A conceptional model of oxygen isotope fractionation and the seasonal cycle of rainfall in the tropics. The values given for the meteoric water source ($\delta^{18}O_{Pre}$) and the amount of rainfall are taken from the isotopic composition of GNIP-station Jakarta and regional climate data sets. "+" and "-" indicate the relative strength and direction of isotopic shifts for relevant processes. (B) Intra-annual $\delta^{18}O$ variations from a teak tree as a function of time of the growing season (Oct-May). The number of sub-sections per ring varied depending on the tree-ring width and the size of dissected wood tissue.

With the beginning of the rainy season increasing rainfall amounts with subsequently lower $\delta^{18}O$ values begin to dilute and lower the initially high $\delta^{18}O$ signal of the soil water (Fig. 5A (2)). At the same time, trees` cambial activity and leaf photosynthesis start (October/November). Altogether, at the beginning of the growing season the uptake of ^{18}O-enriched soil water, in conjunction with enhanced ^{18}O-enrichment of leaf water (driven by transpiration), result in high $\delta^{18}O_{TR}$ values for the first third of each tree ring (Fig. 5B (Max)). However, for a short time at the very beginning of the growing season ^{18}O-enrichment of leaf water may not be a contributing factor as long as young leaves are not fully developed and their stomata are not fully operational. Hence, the initial parenchyma band of teak tree rings is probably not affected by dry season rainfall conditions but from a physiological connection to the previous year growth. If the parenchyma is formed prior to bud burst then its formation relies on stored assimilates carrying the $\delta^{18}O_{TR}$ signature of the previous growing season. Towards the maximum of rainy season (January-March), enhanced condensation processes lead to a progressive depletion in heavy ^{18}O isotopes of rain water, which results in an ^{18}O-depleted soil water signal reaching its lowest $\delta^{18}O$ signature during the peak of the rainy season (Jan-Feb) (Fig. 5A (3)). Soil water evaporation and its related ^{18}O-enrichment are strongly reduced as the soil is shaded from direct insolation by the canopy of the trees. Likewise, the impact of leaf water ^{18}O-enrichment is decreased to a minimum at this time of lowest vapour pressure deficit and highest relative air humidity conditions. This combination of conditions coincides with the low $\delta^{18}O_{TR}$ values found in the middle section of each tree ring (Fig. 5B (Min)). At the end of the rainy season, i.e. growing period, intra-annual tree-ring $\delta^{18}O$ tends to increase again following mainly the isotope trend of the rain water with some modification by ^{18}O-enrichment in leaf water due to evapotranspiration rates that vary with vapour pressure deficit.

The high resolution intra-annual tree-ring $\delta^{18}O$ data indicate that high $\delta^{18}O_{Pre}$ values in dry season are well reflected in the high $\delta^{18}O_{TR}$ values found in the first third of each tree ring (Fig. 5A (2), Fig. 5B (Max)), whereas minimum $\delta^{18}O_{Pre}$ values of the major rainy season are reflected by low $\delta^{18}O_{TR}$ values for the middle part of a tree ring (Fig. 5A (3), Fig. 5B (Min)).

Rainfall amount during the rainy season normally is several times higher than during the dry season and the rainfall signal of rainy season is largely imprinted in the $\delta^{18}O_{TR}$ of two thirds of a tree ring. Thus, the signal of the rainy season should be stronger than the signal of the dry season. However, respective correlations are opposite in sign but of similar magnitude (Fig. 4C). Hence, rainfall conditions persisting during the dry season seem to imply stronger isotopic effects in the tree rings. To verify this hypothesis we analysed the influence of seasonal extremes in rainfall on the annual $\delta^{18}O_{TR}$ values.

4.3. Seasonal extremes in rainfall and their isotopic footprint on $\delta^{18}O_{TR}$ data

A dry season with above average rainfall has a particularly strong influence on tree-ring $\delta^{18}O$ when the following rainy season is rather dry (R^2=0.64, Fig. 6A). Even when followed by a rainy season with rainfall above average the signal of a rather moist dry season is not completely diminished in the annual tree-ring $\delta^{18}O$ (R^2=0.07, Fig. 6B). On the other hand, dry season rainfall variability below average is not reflected in tree-ring $\delta^{18}O$, no matter if the following rainy season is likewise “dry” (Fig. 6C) or “wet” (Fig. 6D). Consequently, the signal of the rainy season is well expressed when the preceding dry season was rather dry (Fig. 6E). Interestingly, a dry season with above average rainfall apparently strengthens the signal of a rainy season with below average rainfall in tree-ring $\delta^{18}O$ (R^2=0.63, Fig. 6F). In general, a dry season with enhanced ^{18}O-enriched rainfall sets a high initial $\delta^{18}O$-

source level. Hence, a following rainy period with reduced rain, and a less than normal ^{18}O-depleted signature, is only partly diluting the ^{18}O-enrichment signal of dry season`s rain. The extent to which a "wet" dry season signal is overwritten depends on the rainfall amount during the rainy season. This leads us to the conclusion that the annual $\delta^{18}O_{TR}$ record cannot give unambiguous information about rainfall conditions during individual seasons (dry and rainy season). However, the seasonality, the difference between dry and rainy season rainfall amount, does show a high correlation (r=0.53; Fig. 4C). The rainfall signal from dry or rainy season is damped in the tree-ring $\delta^{18}O$ values due to seasonally alternating isotope signatures in $\delta^{18}O_{Pre}$. Only high-resolution $\delta^{18}O_{TR}$ records seem to provide detailed information about both, the dry and rainy season rainfall variability.

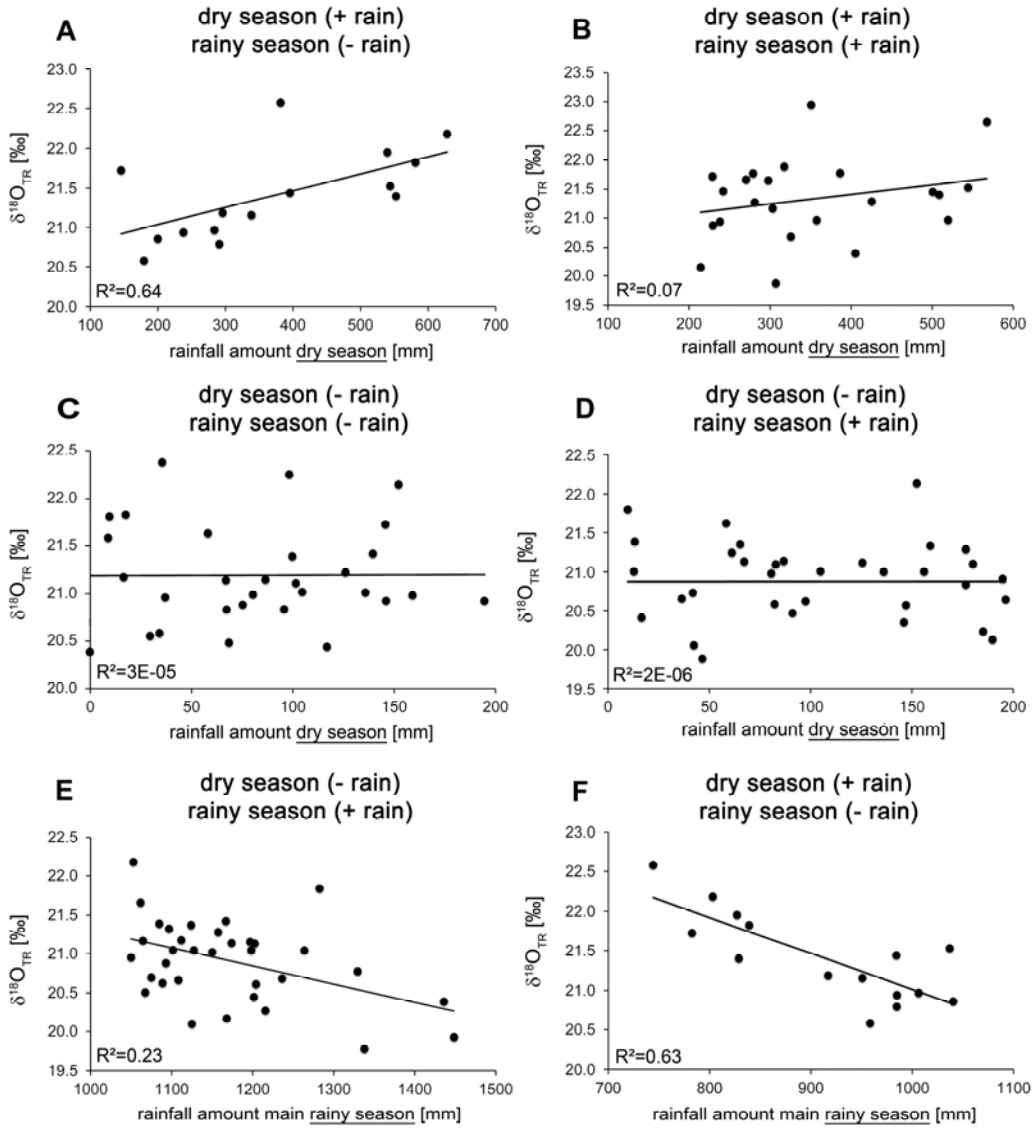

Fig. 6. Comparison of the influence of different rainfall conditions during dry and rainy season on the tree-ring $\delta^{18}O$ values. ''+'' and ''-'' represent below or above average rainfall amount for corresponding season. A dry season with above average rainfall has a strong influence on $\delta^{18}O_{TR}$ when the following rainy season is rather dry (A), but is weakly reflected when the following rainy season has above average rainfall (B). A dry season with below average rainfall is not reflected in $\delta^{18}O_{TR}$, no matter if the following rainy season is likewise drier (C) or wetter (D) than average. The signal of the rainy season is well expressed when the preceding dry season was rather dry (E).

Interestingly, a dry season with above average rainfall apparently strengthens the signal of a rainy with below average rainfall $\delta^{18}O_{TR}$ (F). See text for further details.

Previous $\delta^{18}O$ teak studies from Indonesia on two cores showed a common climate influence on inter-annual scale for time period 1950-1980 (Poussart et al., 2004). Poussart et al.´s intra-annual $\delta^{18}O$ analyses for the same time span showed a similar pattern as we found with a maximum early in the growing season, followed by a gradual decrease and often a sharp increase towards the end of the growing season. However, in their study a correlation with local or regional rainfall pattern was not tested in detail. $\delta^{18}O$ studies on teak from India (Managave et al., 2010a; Managave et al., 2011) found both negative and positive correlations with the amount of rainy season rainfall at inter- and intra-annual scale. Studies in tropical regions of South-America have likewise reported negative correlation with the rainfall amount during rainy season (Ballantyne et al., 2010; Brienen et al., 2012), as have isotope studies in Southeast Asia (Sano et al., 2012; Xu et al., 2011; Zhu et al., 2012). However, none reported correlations with dry and rainy season rainfall as revealed here for Indonesian teak.

5. Conclusions and perspectives

We tested the dendroclimatological potential of multiple, centennial, tree-ring records (ring width, $\delta^{13}C_{TR}$ and $\delta^{18}O_{TR}$) of *Tectona grandis* in Central Java. All three tree-ring records revealed a seasonal rainfall signal, but for different time intervals and with different stability in time. As shown in previous studies tree-ring widths correlate positively with transitional months of the monsoon (e.g. D'Arrigo et al., 1994). Newly developed stable isotope records show a higher degree of common forcing and display a significant negative correlation with rainy season precipitation. In addition, our $\delta^{18}O_{TR}$ revealed a positive correlation with dry season rainfall. These relationships of opposite signs reflect a distinct seasonal contrast of the $\delta^{18}O_{Pre}$ signature of Central Java rainfall variability. Thus the formation of tree-ring $\delta^{18}O$ is related to dry and rainy season pattern, whereas the main rainy season signal is dominant and stable in time. However, the dry season has a weakening effect on the main rainy season $\delta^{18}O_{Pre}$ signal depending on the respective seasonal rainfall conditions. High-resolution $\delta^{18}O_{TR}$ records permit to disentangle the seasonal cycle of $\delta^{18}O$ in rainfall.

We have shown that stable isotope records from Indonesian teak offer additional information to climate investigations. However, to distinguish seasonal rainfall variability across the tropical Indo-Pacific region further studies need to focus on high-resolution stable isotope studies. Long-term reconstruction of annual rainfall variability (rainy and dry season rainfall), including unusual rainfall anomalies such as during ENSO events, may be possible with tree-ring $\delta^{18}O$ and could improve our understanding of the Asian monsoon system. Such studies will be promoted by novel methods like UV-Laser micro-dissection sampling that enable sample preparation with the highest precision able to accommodate tree-ring samples with large variations in ring-width and irregular shape of tree-ring boundaries.

Acknowledgments

This study was supported by the CADY (BMBF, 03G0813H), the HIMPAC (DFG, HE 3089/4-1) and the INDOPAL (HE3089/1-1) projects. We thank Tomy Listyanto and Navis Rofii for their assistance in the field work. Heiko Baschek, Carmen Bürger and David Göhring are thanked for support in the

laboratory and Isabel Dorado and Katja Fregien for fruitful discussions. Furthermore, we are also grateful to two anonymous reviewers for their constructive and helpful comments.

Appendix A. Supplementary data

Supplementary data related to this article can be found at http://dx.doi.org/10.1016/j.quascirev.2013.05.018.

References

Aldrian, E., Susanto, R.D., 2003. Identification of three dominant rainfall regions within indonesia and their relationship to sea surface temperature. International Journal of Climatology 23, 1435-1452.

Araguás-Araguás, L., Froehlich, K., Rozanski, K., 1998. Stable isotope composition of precipitation over southeast Asia. Journal of Geophysical Research-Atmospheres 103, 28721-28742.

Araguás-Araguás, L., Froehlich, K., Rozanski, K., 2000. Deuterium and oxygen-18 isotope composition of precipitation and atmospheric moisture. Hydrological Processes 14, 1341-1355.

Ballantyne, A.P., Baker, P.A., Chambers, J.Q., Villalba, R., Argollo, J., 2010. Regional Differences in South American Monsoon Precipitation Inferred from the Growth and Isotopic Composition of Tropical Trees. Earth Interactions 15, 1-35.

Barbour, M.M., 2007. Stable oxygen isotope composition of plant tissue: a review. Functional Plant Biology 34, 83-94.

Berlage, H.P., 1931. On the relationship between thickness of tree rings of Djati (teak) trees and rainfall on Java. Tectona.

Boer, R.A.R.S., 2005. Agriculture drought in Indonesia, In: Boken, V.K., Cracknell, A.P., Heathcote, R.L. (Eds.), Monitoring and predicting agriculture drought: A global study, New York, pp. 330-344.

Borella, S., Leuenberger, M., Saurer, M., Siegwolf, R., 1998. Reducing uncertainties in $\delta^{13}C$ analysis of tree rings: Pooling, milling, and cellulose extraction. Journal of Geophysical Research-Atmospheres 103, 19519-19526.

Borgaonkar, H.P., Sikder, A.B., Ram, S., Pant, G.B., 2010. El Niño and related monsoon drought signals in 523-year-long ring width records of teak (*Tectona grandis* L.F.) trees from south India. Palaeogeography, Palaeoclimatology, Palaeoecology 285, 74-84.

Braak, C., 1921-29. The climate of the Netherlands Indies. Meded. En Verh. Koninklijk Magnetisch en Meteorologisch Oberservatorium te Batavia 8, 257.

Brienen, R., Wanek, W., Hietz, P., 2011. Stable carbon isotopes in tree rings indicate improved water use efficiency and drought responses of a tropical dry forest tree species. Trees - Structure and Function 25, 103-113.

Brienen, R.J.W., Helle, G., Pons, T.L., Guyot, J.L., Gloor, M., 2012. Oxygen isotopes in tree rings are a good proxy for Amazon precipitation and El Niño-Southern Oscillation variability. Proceedings of the National Academy of Sciences 109, 16957-16962.

Briffa, K., Jones, B., 1990. Basic chronology statistics and assessment, In: Cook, A.C., Briffa, K., Kairiukstis, L.A. (Eds.), Methods of Dendrochronology - Applications in the Environmental Sciences. Kluwer Academic Publ., Dordrecht, pp. 137-152.

Buckley, B.M., Palakit, K., Duangsathaporn, K., Sanguantham, P., Prasomsin, P., 2007. Decadal scale droughts over northwestern Thailand over the past 448 years: links to the tropical Pacific and Indian Ocean sectors. Climate Dynamics 29, 63–71.

Cernusak, L.A., Aranda, J., Marshall, J.D., Winter, K., 2007. Large variation in whole-plant water-use efficiency among tropical tree species. New Phytologist 173, 294-305.

Cook, E., Kairiukstis, L.A., 1990. Methods of Dendrochronology. Applications in the Environmental Sciences. Kluwer, Dordrecht.

Cook, E.R., Krusic, P.J., Peters, K., Holmes, R., 2012. Program ARSTAN version 41 (http://www.ldeo.columbia.edu/tree-ring-laboratory/resources/software).

Cook, E.R., Peters, K., 1981. The smoothing spline: a new approach to standardizing forest interior tree-ring width series for dendroclimatic studies. Tree-Ring Bulletin 41, 45-53.

Coster, C., 1927. Zur Anatomie und Physiologie der Zuwachszonen- und Jahresringbildung in den Tropen. Ann. Jard. Bot. Buitenzong 37, 49-160.

Coster, C., 1928. Zur Anatomie und Physiologie der Zuwachszonen- und Jahresringbildung in den Tropen. Ann. Jard. Bot. Buitenzong 38, 1-114.

Craig, H., 1957. Isotopic standards for carbon and oxygen and correction factors for mass-spectrometric analysis of carbon dioxide. Geochimica et Cosmochimica Acta 12, 133-149.

Cropper, J.P., 1979. Tree-ring skeleton plotting by computer. Tree-ring Bulletin 39, 47-59.
D'Arrigo, R., Jacoby, G.C., Krusic, P., 1994. Progress in dendroclimatic studies in Indonesia. Terrestrial, Atmospheric and Oceanic Sciences 5, 349-363.
D'Arrigo, R., Wilson, R., Palmer, J., Krusic, P., Curtis, A., Sakulich, J., Bijaksana, S., Zulaikah, S., Ngkoimani, L.O., 2006a. Monsoon drought over Java, Indonesia, during the past two centuries. Geophysical Research Letters 33, L04709.
D'Arrigo, R., Wilson, R., Palmer, J., Krusic, P., Curtis, A., Sakulich, J., Bijaksana, S., Zulaikah, S., Ngkoimani, L.O., Tudhope, A., 2006b. The reconstructed Indonesian warm pool sea surface temperatures from tree rings and corals: Linkages to Asian monsoon drought and El Niño–Southern Oscillation. Paleoceanography 21, PA3005.
Dansgaard, W., 1964. Stable isotopes in precipitation. Tellus 16, 437-468.
DeBoer, H.J., 1951. Treering measurements and weather Fluctuations in Java from A.D. 1514. Proc.K.Ned.Akad.Wetensch. 54, 194-209.
Douglass, A.E., 1935. Dating Pueblo Bonito and Other Ruins of the Southwest, Nat. Geog. Soc. Pueblo Bonito Series, Washington, D.C.
Esper, J., Neuwirth, B., Treydte, K., 2001. A new parameter to evaluate temporal signal strength of tree-ring chronologies. Dendrochronologia 19, 93-102.
Evans, M.N., 2007. Toward forward modeling for paleoclimatic proxy signal calibration: A case study with oxygen isotopic composition of tropical woods. Geochemistry Geophysics Geosystems 8, Q07008.
Evans, M.N., Cane, M.A., Schrag, D.P., Kaplan, A., Linsley, B.K., Villalba, R., Wellington, G.M., 2001. Support for tropically-driven pacific decadal variability based on paleoproxy evidence. Geophysical Research Letters 28, 3689-3692.
Evans, M.N., Schrag, D.P., 2004. A stable isotope-based approach to tropical dendroclimatology. Geochimica et Cosmochimica Acta 68, 3295-3305.
Farquhar, G.D., O'Leary, M.H., Berry, J.A., 1982. On the Relationship between Carbon Isotope - Discrimination and the Intercellular - Carbon Dioxide Concentration in Leaves. Aust. J. Plant Physiol. 9, 121-137.
Feng, X., Epstein, S., 1995. Carbon isotopes of trees from arid environments and implications for reconstructing atmospheric CO_2 concentrations. Geochimica et Cosmochimica Acta 59, 2599-2608.
Fichtler, E., Helle, G., Worbes, M., 2010. Stable-Carbon Isotope Time Series from Tropical Tree Rings Indicate a Precipitation Signal. Tree-Ring Research 66, 35-49.
Fritts, H.C., 1976. Tree Rings and Climate. Cambridge University Press, Cambridge, London.
Gärtner, H., Nievergelt, D., 2010. The core-microtome: A new tool for surface preparation on cores and time series analysis of varying cell parameters. Dendrochronologia 28, 85-92.
Gat, J.R., 1996. Oxygen and hydrogen isotopes in the hydrologic cycle. Annu. Rev. Earth Planet. Sci. 24, 225-262.
Gebrekirstos, A., Worbes, M., Teketay, D., Fetene, M., Mitlöhner, R., 2009. Stable carbon isotope ratios in tree rings of co-occurring species from semi-arid tropics in Africa: Patterns and climatic signals. Global and Planetary Change 66, 253-260.
Geiger, F., 1915. Anatomische Untersuchungen über die Jahresringbildung von Tectona grandis, In: Pfeffer, W. (Ed.), Jahrbücher für wissenschaftliche Botanik.
Hackert, E.C., Hastenrath, S., 1986. Mechanisms of Java Rainfall Anomalies. Monthly Weather Review 114, 745-757.
Hastenrath, S., 1991. Rainfall Anomalies in Indonesia, Climate dynamics of the tropics.
Helle, G., Schleser, G.H., 2004a. Beyond CO_2-fixation by Rubisco – an interpretation of $^{13}C/^{12}C$ variations in tree rings from novel intra-seasonal studies on broad-leaf trees. Plant, Cell and Environment 27, 367-380.
Helle, G., Schleser, G.H., 2004b. Interpreting climate proxies from tree-rings, In: Fischer, H., Floeser, G., Kumke,T., Lohmann, G., Miller, H., Negendank, J.F.W., von Storch, H. (Ed.), The KIHZ project: Towards a synthesis of Holocene proxy data and climate models, pp. 129-148.

Hietz, P., Wanek, W., Dunisch, O., 2005. Long-term trends in cellulose $\delta^{13}C$ and water-use efficiency of tropical Cedrela and Swietenia from Brazil. Tree Physiology 25, 745-752.

Holmes, R.L., 1983. Computer-assisted quality control in tree-ring dating and measurement. Tree-Ring Bulletin 43 69-78.

Hughes, M.K., 2011. Dendroclimatology in High-Resolution Paleoclimatology, In: Hughes, M.K., Swetnam, T.W., Diaz, H.F. (Eds.), Dendroclimatology. Springer Netherlands, pp. 17-34.

Jacoby, G.C., D'Arrigo, R.D., 1990. Teak (*Tectona grandis* L.F.), a tropical species of large-scale dendroclimatic potential. Dendrochronologia 8, 83-98.

Jones, P.D., Hulme, M., 1996. Calculating regional climatic time series for temperature and precipitation: Methods and illustrations. International Journal of Climatology 16, 361-377.

Kürschner, W.M., van der Burgh, J., Visscher, H., Dilcher, D.L., 1996. Oak leaves as biosensors of late neogene and early pleistocene paleoatmospheric CO_2 concentrations. Marine Micropaleontology 27, 299-312.

Leavitt, S.W., 2010. Tree-ring C–H–O isotope variability and sampling. Science of the Total Environment 408, 5244-5253.

Leuenberger, M., 2007. To what extent can ice core data contribute to the understanding of plant ecological developments of the past?, In: Dawson, T., Siegwolf, R. (Eds.), Stable isotopes as indicators of ecological change. Academic Press, London, pp. 211-234.

Managave, S.R., Sheshshayee, M., Bhattacharyya, A., Ramesh, R., 2010a. Intra-annual variations of teak cellulose $\delta^{18}O$ in Kerala, India: implications to the reconstruction of past summer and winter monsoon rains. Climate Dynamics, 1-13.

Managave, S.R., Sheshshayee, M.S., Borgaonkar, H.P., Ramesh, R., 2010b. Past break-monsoon conditions detectable by high resolution intra-annual $\delta^{18}O$ analysis of teak rings. Geophysical Research Letters 37, L05702.

Managave, S.R., Sheshshayee, M.S., Ramesh, R., Borgaonkar, H.P., Shah, S.K., Bhattacharyya, A., 2011. Response of cellulose oxygen isotope values of teak trees in differing monsoon environments to monsoon rainfall. Dendrochronologia 29, 89-97.

McBride, J., 1999. Indonesia, Papua New Guinea, and tropical Australia: the southern hemisphere monsoon, In: Karoly, D., Vincen, t.D. (Eds.), Meteorology of Southern Hemisphere, Boston, pp. 89-98.

McCarroll, D., Loader, N.J., 2004. Stable isotopes in tree rings. Quaternary Science Reviews 23, 771-801.

Mitchell, T.D., Jones, P.D., 2005. An improved method of constructing a database of monthly climate observations and associated high-resolution grids. International Journal of Climatology 25, 693-712.

Murphy, J.O., Whetton, P.H., Ritsema, A.R., 1989. A re-analysis of a tree ring chronology from Java. North-Holland, Amsterdam.

Nock, C.A., Baker, P.J., Wanek, W., Leis, A., Grabner, M., Bunyavejchewin, S., Hietz, P., 2011. Long-term increases in intrinsic water-use efficiency do not lead to increased stem growth in a tropical monsoon forest in western Thailand. Global Change Biology 17, 1049-1063.

Poussart, P.F., Evans, M.N., Schrag, D.P., 2004. Resolving seasonality in tropical trees: multi-decade, high-resolution oxygen and carbon isotope records from Indonesia and Thailand. Earth and Planetary Science Letters 218, 301-316.

Pumijumnong, N., Eckstein, D., Sass, U., 1995. Tree-ring research on *Tectona grandis* on northern Thailand. Iawa Journal 16, 385-392.

Ram, S., Borgaonkar, H., Sikder, A., 2008. Tree-ring analysis of teak (*Tectona grandis* L.F.) in central India and its relationship with rainfall and moisture index. Journal of Earth System Science 117, 637-645.

Riemer, T., 1994. Über die Varianz von Jahrringbreiten. Statistische Methoden für die Auswertung der jährlichen Dickenzuwächse von Bäumen unter sich ändernden Lebensbedingungen. Berichte des Forschungszentrums Waldökosysteme 121. Göttingen.

Rinn, F., 2005. TSAP - WinTM. Time Series Analysis and Presentation for Dendrochronology and Related Applications. Version 4.6, Heidelberg.

Roden, J.S., Lin, G., Ehleringer, J.R., 2000. A mechanistic model for interpretation of hydrogen and oxygen isotope ratios in tree-ring cellulose. Geochimica et Cosmochimica Acta 64, 21-35.

Sano, M., Xu, C., Nakatsuka, T., 2012. A 300-year Vietnam hydroclimate and ENSO variability record reconstructed from tree ring $\delta^{18}O$. Journal of Geophysical Research 117, D12115.

Sarachik, E.S., Cane, M.A., 2010. The El Niño-Southern Oscillation Phenomenon. Cambridge University Press.

Schubert, B.A., Jahren, A.H., 2012. The effect of atmospheric CO_2 concentration on carbon isotope fractionation in C_3 land plants. Geochimica et Cosmochimica Acta 96, 29-43.

Schulman, E., 1956. Dendroclimatic Change in Semiarid America. University of Arizona Press, Tuscon, Arizona.

Schweingruber, F.H., 1983. Der Jahrring: Standort, Methodik, Zeit und Klima in der Dendrochronologie. Paul Haupt, Bern.

Schweingruber, F.H., Eckstein, D., Serre-Bachet, F., Bräker, O.U., 1990. Identification, presentation and interpretation of event years and pointer years in dendrochronology. Dendrochronologia 8, 9-38.

Shah, S.K., Bhattacharyya, A., Chaudhary, V., 2007. Reconstruction of June–September precipitation based on tree-ring data of teak (*Tectona grandis* L.) from Hoshangabad, Madhya Pradesh, India. Dendrochronologia 25, 57-64.

Stokes, M.A., Smiley, T.L., 1968. An Introduction to Tree-ring Dating. University of Arizona Press, Tuscon.

Sukanto, M., 1969. Climate of Indonesia, In: Arakawa, H. (Ed.), Climate of Northern and Eastern Asia.

Taylor, A.M., Renée Brooks, J., Lachenbruch, B., Morrell, J.J., Voelker, S., 2008. Correlation of carbon isotope ratios in the cellulose and wood extractives of Douglas-fir. Dendrochronologia 26, 125-131.

Ummenhofer, C., D'Arrigo, R., Anchukaitis, K., Buckley, B., Cook, E., 2013. Links between Indo-Pacific climate variability and drought in the Monsoon Asia Drought Atlas. Climate Dynamics 40, 1319-1334.

Verheyden, A., Roggeman, M., Bouillon, S., Elskens, M., Beeckman, H., Koedam, N., 2005. Comparison between $\delta^{13}C$ of α-cellulose and bulk wood in the mangrove tree *Rhizophora mucronata*: Implications for dendrochemistry. Chemical Geology 219, 275-282.

Walter, H., Breckle, S.W., 1991. Ökologische Grundlagen in globaler Sicht. Fischer, Stuttgart.

Wieloch, T., Helle, G., Heinrich, I., Voigt, M., Schyma, P., 2011. A novel device for batch-wise isolation of α-cellulose from small-amount wholewood samples. Dendrochronologia 29, 115-117.

Wigley, T.M.L., Briffa, K.R., Jones, P.D., 1984. On the Average Value of Correlated Time-Series, with Applications in Dendroclimatology and Hydrometeorology. Journal of Climate and Applied Meteorology 23, 201-213.

Xu, C., Sano, M., Nakatsuka, T., 2011. Tree ring cellulose $\delta^{18}O$ of *Fokienia hodginsii* in northern Laos: A promising proxy to reconstruct ENSO? Journal of Geophysical Research 116, D24109.

Zhu, M., Stott, L., Buckley, B., Yoshimura, K., Ra, K., 2012. Indo-Pacific Warm Pool convection and ENSO since 1867 derived from Cambodian pine tree cellulose oxygen isotopes. Journal of Geophysical Research 117, D11307.

Appendix A. Supplementary data

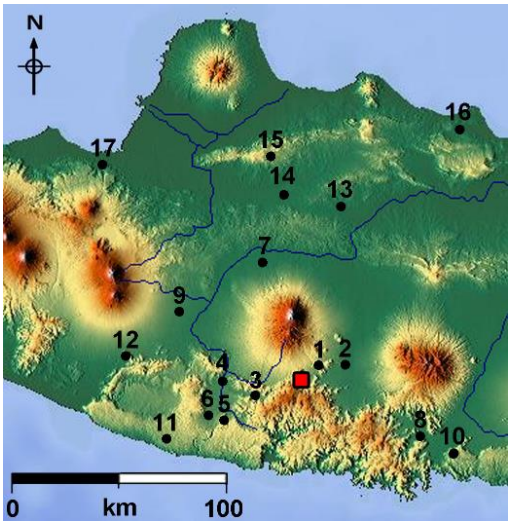

Fig. A. Map of Central/Eastern Java indicating the study site (red triangle) and climate stations with rainfall data (black dots).

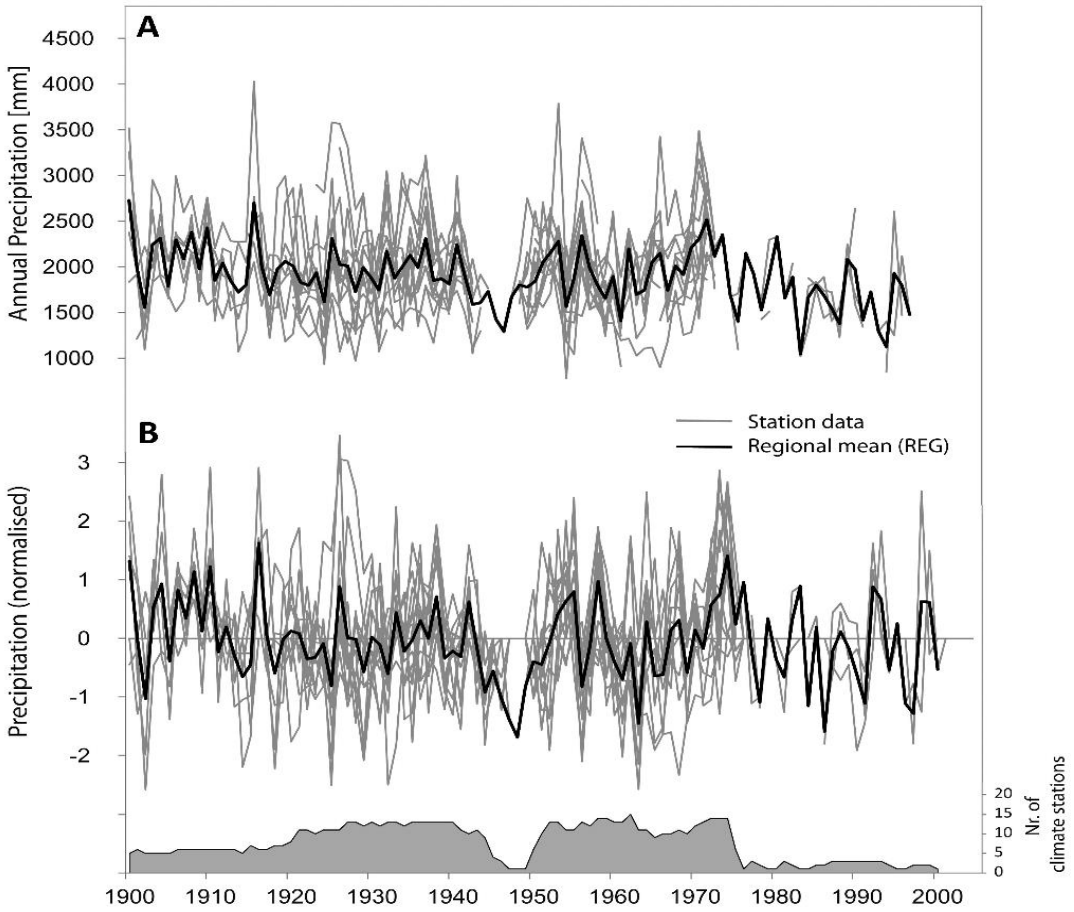

Fig. B. Annual (July to June) rainfall data from climate stations (Table S1); (A) rainfall means; (B) data normalized over individual series lengths, mean of this series (REG) and number of series contributing to the mean.

Table A. Climate stations with rainfall data used for calculating of regional rainfall mean (REG).

Climate station	Nr.	Coordinates	Altitude (m)	Time period	Distance to study site (km)
Purwantoro	1	-7.85N, 111.27E	500	1905-1975	10
Sungkur	2	-7.85N, 111.38E	95	1920-1975	20
Batuwarno	3	-7.98N, 110.01E	380	1944-1996	20
Wuryantoro	4	-7.90N, 110.87E	180	1920-1975	35
Giritontro	5	-8.08N, 110.86E	280	1944-2002	40
Pracimantoro	6	-8.05N, 110.81E	450	1944-2002	45
Mojo	7	-7.43N, 110.05E	85	1926-1975	50
Bendo	8	-8.15N, 111.68E	120	1900-1975	60
Delanggu	9	-7.62N, 110.70E	130	1900-1975	60
Tumpakmergo	10	-8.23N, 111.82E	88	1926-1975	70
Ngranti	11	-8.15N, 110.63E	300	1920-1971	70
Tanjungtirto	12	-7.80N, 110.47E	115	1900-1975	80
Randublatung	13	-7.20N, 111.38E	55	1915-1975	80
Nglangon	14	-7.15N, 111.15E	80	1900-1975	85
Karangasem	15	-7.00N, 111.10E	158	1900-1975	100
Kerek	16	-6.90N, 111.88E	110	1900-1975	130
Semarang	17	-7.00N, 110.40E	3	1957-2003	130